pubs.acs.org/Biomac

Article

Bacterial-Infection-Triggered Release of Antibacterial Aldehyde from Triblock Copolyether Hydrogels

Neha Choudhury,[§] Seongeun Cho,[§] Jinsu Baek, Jinkee Hong,* and Byeong-Su Kim*

Cite This: https://doi.org/10.1021/acs.biomac.4c00586

Read Online

ACCESS | Metrics & More | Article Recommendations | Supporting Information

ABSTRACT: Bacterial infections pose a significant threat to public health worldwide. Hydrogel-based biomaterials have proven to be particularly useful in addressing persistent bacterial infections due to their stimuli-responsive degradability, high biocompatibility, ability to release antibacterial agents on demand, and long-lasting antibacterial activity. Herein, we fabricated ABA-type triblock copolyether hydrogels, wherein, hexanal, a bioactive aldehyde with antibacterial activity, was affixed to the hydrophobic micellar core via acetal linkage. The hydrogel exhibited degradation under acidic environment via the hydrolysis of acetal linkages, leading to the concomitant release of hexanal to exhibit highly potent bactericidal activity against both *Escherichia coli* and *Staphylococcus aureus*. Furthermore, a dual-mode release of the model therapeutic agent Nile Red from the hydrophobic micellar core of the hydrogel in conjunction with hexanal was demonstrated using this system. We anticipate that this study will provide a new platform for the development of hydrogels with tailorable release profiles for biologically active compounds that are activated by the acidification triggered by bacterial infection.

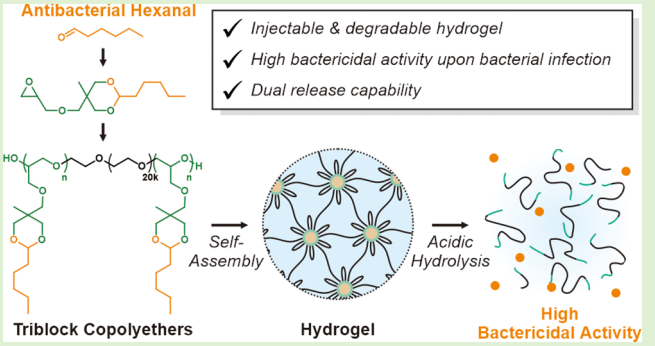

INTRODUCTION

Bacterial infections remain a persistent threat to human health because bacteria can quickly spread and infect a population either through direct contact with an infected individual or via contact with contaminated objects.[1] Even with the progress in medicine and public health, antibiotic-resistant bacteria have become a significant threat to global health.[2] To address this issue, antibiotics, polymeric materials, antibacterial peptide mimetics, and semisynthetic antibiotics have been developed as alternative therapeutic strategies.[3−6] However, many of these systems are limited by their toxicity, difficult administration process, limited spectrum activity and water solubility, resistance to antibiotic-resistant pathogens, premature exhaustion of antibiotics, and/or high manufacturing costs.[7]

One effective treatment that has emerged recently is the use of antibacterial hydrogels, which offer strong bacterial inhibition, cell adhesion capability, and high biocompatibility.[8] Hydrogels are three-dimensional (3D), hydrophilic polymer networks with a high water or biological fluid absorption capacity that are fabricated from natural or synthetic polymers via physical or chemical cross-linking.[9,10] In particular, injectable hydrogels have been used for the controllable and target-specific release of antibacterial agents that are loaded into the hydrogel matrix.[11] Notably, stimuli-responsive antibacterial hydrogels have attracted significant attention due to their ability to modulate the release of antimicrobial agents and activate them on demand in response to bacterial metabolites stimuli.[12,13] Bacterial metabolites stimuli refer to alterations in the local microenvironment induced by the rapid growth and colonization of bacteria at the site of infection, including the secretion of acids, enzymes, and oxidative stress factors.[14] This capability enables a fine balance between biocompatibility and antibacterial efficacy and prevents early depletion of antimicrobial agents. This has attracted much interest by endowing self-adaptive antibacterial activity to hydrogels.

Among the wide spectrum of bacterial metabolites stimuli, pH changes indicate the acidification of the infected microenvironment (pH 4.5−6.5) due to bacterial secretion of compounds such as lactic acid, acetic acid, and malic acid.[12,15] Consequently, in recent years, pH-responsive linkages have been incorporated into antibacterial hydrogel, facilitating the development of adaptive antibacterial hydrogels that release or expose antimicrobial agents through the degradation of these linkages in response to pH changes.[16,17] Wang and co-workers created a pH-responsive antimicrobial hydrogel with nanofiber networks by self-assembling octapeptides at neutral pH for treating methicillin-resistant *Staphylococcus aureus* (MRSA)-

Received: May 1, 2024
Revised: June 28, 2024
Accepted: June 28, 2024

infected wounds in diabetic mice; under acidic conditions, the hydrogel destabilized, releasing octapeptides and activating their antimicrobial properties.[18] Another study designed a pH-responsive injectable nanocomposite hydrogel as a long-lasting implant for cancer therapy, loading it with a doxorubicin prodrug that releases the drug sustainably over a month in acidic tumor environments due to hydrazone bond cleavage.[19]

Several pH-sensitive linkers, including Schiff bases, hydrazones, and carbonates, have been employed, but acetals have drawn considerable interest because they produce charge-neutral byproducts upon cleavage.[20,21] Despite the benefits of acetal linkages, there are very few studies in the literature that have investigated the utility of these functionalities in the design of degradable polymeric biomaterials and hydrogels. In this context, our group has designed a range of functional epoxide monomers with acetal linkages as the pH-responsive hydrophobic block in smart drug delivery systems.[21−23] The self-assembled polymeric micelles composed of these epoxide monomers exhibited pH-responsive degradation under acidic conditions due to the hydrolysis of the acetal linkages.

On the other hand, ABA-type triblock copolymer hydrogels, consisting of hydrophobic A end-blocks and a hydrophilic B midblock, have been the subject of extensive research due to their unique properties and versatility in drug delivery systems.[24] Upon dissolution in water, the hydrophilic blocks of these copolymers form physical cross-links to create a three-dimensional (3D) hydrogel network.[25] Their advantage lies in the capability to control properties by altering block composition and polymerization degree, facilitating the creation of hydrogels with diverse mechanical properties and tunable degradation rates. In a recent study, we fabricated ABA-type triblock copolymer hydrogels with a poly(ethylene glycol) (PEG) midblock and A-blocks containing acetal pendants that degrade in an acidic environment, resulting in a gel-to-sol transition at room temperature with a tailorable viscoelastic transition.[26,27] It will thus be possible to incorporate a bioactive agent into the polymeric hydrogel via cleavable linkages that release the agent in response to external stimuli. While PEG is frequently utilized in biomedical applications because of its biocompatibility and hydrophilicity, certain studies indicate that it might provoke immune responses in some individuals, perhaps leading to the formation of anti-PEG antibodies. However, upon conjugation to macromolecules, they could become nonimmunogenic.[28] A recent study found that PEGs are effective cryoprotectants for mesenchymal stem cells, with their efficacy influenced by factors such as molecular weight, cell permeability, and localization.[29]

Volatile antimicrobial agents such as low-molecular-weight fatty acids, aldehydes, and essential oils are known to exhibit high antimicrobial activity.[30] Among these agents, hexanal has been approved by the US Food and Drug Administration for use as a food additive and has demonstrated antimicrobial activity against various microorganisms.[31−33] Hexanal acts by disrupting the cell membrane of microorganisms and interfering with their metabolic processes, leading to cellular death. However, the use of highly volatile substances such as hexanal has been limited to date, and there remains wide scope for the development of effective systems for the regulated release of volatile active substances.

Herein, we design and synthesize the polyether-based ABA-type triblock copolymer hydrogels bearing PEG midblock and hydrophobic end-blocks to which a bioactive aldehyde with potential antibacterial activity was affixed via pH-responsive acetal linkages. Initially, a series of triblock copolymers with varying degrees of polymerization for the A end-blocks were fabricated via the anionic ring-opening polymerization (AROP) of functional epoxide monomers. When dispersed in water above a critical polymer concentration, these triblock copolyethers formed hydrogels. The triggered release of the bioactive aldehyde from the hydrogels was then observed under acidic conditions through the hydrolysis of the acetal pendants with the subsequent gel-to-sol transition of the hydrogel. Most importantly, the hexanal released from the ABA triblock copolymer hydrogel exhibited high antibacterial activity against *Escherichia coli* and *S. aureus*, while retaining the low cytotoxicity of the triblock copolymer after the release of hexanal even at high concentrations. Furthermore, by exploiting the hydrophobic micellar core of the hydrogel cross-linking junction, a model hydrophobic therapeutic agent was encapsulated in the hydrogel. Under acidic conditions, the breaking of the acid-labile acetal linkages led to the controlled release of the bioactive aldehyde and the degradation of the hydrogel, thereby promoting the release of the encapsulated therapeutic agent. Thus, our system enables the simultaneous release of a bioactive aldehyde and a model therapeutic agent from the hydrogel at acidic pH, which can be readily extended to the use of other bioactive compounds. Consequently, this hydrogel possesses antibacterial properties activated by the acidification triggered by bacterial infection, facilitating the on-demand release of antimicrobial agents and adaptively killing bacteria. It reduces the risk of premature depletion of antimicrobials while minimizing unintended cytotoxic effects on host cells from continuous exposure to antimicrobials. Coupled with its high biological activity, the antibacterial hydrogel developed in this study represents a promising approach for the treatment of bacterial infections.

EXPERIMENTAL SECTION

Materials. Hexanal (98%), *p*-toluenesulfonic acid monohydrate (*p*-TsOH, > 98%), 1,1,1-tris(hydroxymethyl)ethane, poly(ethylene glycol) (PEG_{20K}, average M_n = 20 kDa), acetonitrile (anhydrous), phosphazene base *t*-Bu-P_4 solution in *n*-hexane (0.8 M), tetrabutylammonium bromide (TBAB, reagent plus 99%), Nile Red, and benzoic acid (99.5%) were purchased from Sigma-Aldrich and used as received. Triethylamine (TEA, 99%) and epichlorohydrin (>99%) were purchased from TCI. Toluene was dried and degassed using a solvent purifier (Vacuum Atmospheres) and used immediately after collection. Dichloromethane (DCM), *N*,*N*-dimethylformamide (DMF), dimethyl sulfoxide (DMSO), tetrahydrofuran (THF), diethyl ether, ethyl acetate, hexane, and methanol (MeOH) were purchased from SK Chemicals. The deuterated NMR solvent $CDCl_3$ and methanol-d_4 were obtained from Cambridge Isotope Laboratories, Inc.

Characterization. All ^{1}H NMR spectra were recorded on a Bruker 300 and 400 MHz spectrometer at 25 °C. The ^{13}C and heteronuclear single-quantum correlation (HSQC) NMR spectra were also recorded on a Bruker 400 MHz spectrometer at 25 °C. $CDCl_3$ and methanol-d_4 were used as internal standards. The number and weight averages (M_n and M_w) and the corresponding molecular weight distribution ($Đ$, M_w/M_n) of the polymer samples were measured using gel permeation chromatography (GPC) with an Agilent 1200 Series HPLC system and THF as the eluent at 25 °C and a flow rate of 1.00 mL/min with a refractive index (RI) detector. All calibrations were conducted using PEG standards. Differential scanning calorimetry (DSC) (Q200 model, TA Instruments) was employed under a nitrogen atmosphere from −80 to 200 °C with a heating rate of 10 °C/min. The samples were annealed prior to measurement, and the second cycle was used to assess the thermal

https://doi.org/10.1021/acs.biomac.4c00586
Biomacromolecules XXXX, XXX, XXX−XXX

characteristics of the resulting polymers. A TFD8501 freeze-dryer (Ilshin BioBase) was used to lyophilize the hydrogel samples. The microstructural evolution of the hydrogel samples before and after degradation at pH 5.0 was investigated using a scanning electron microscope (SEM) (JSM-IT500HR) at an accelerating voltage of 20 kV. Rheological analysis of the hydrogel was carried out on an Anton Parr MCR302 rheometer equipped with a parallel plate geometry (diameter: 50 mm). Hydrogel samples were loaded with a 0.6 mm gap between the Peltier-controlled thermostat plates. To reduce water evaporation during the measurements, water was poured around the sample stage, which was subsequently covered with a solvent trap. A frequency range of 0.1−100 rad/s at 37 °C was used for the oscillatory shear experiments.

Synthesis of Protected Hexanal. Typically, 36.0 g (299.52 mmol) of tris(hydroxymethyl)ethane was added to a 250 mL round-bottom flask and dissolved in 150 mL of THF. The solution was then treated with 10.0 g (99.84 mmol) of hexanal and 95 mg (0.49 mmol) of *p*-TsOH and refluxed in an oil bath at 70 °C for 12 h. After 12 h, the mixture was cooled down to room temperature, and 1.6 mg (15.97 mmol) of TEA was added to quench the reaction. In the next step, THF was evaporated under reduced pressure, and the residue was extracted with ethyl acetate. The organic layer was subsequently washed three times with a brine solution and dried over anhydrous Na_2SO_4. The extract was concentrated under reduced pressure and the crude product was purified using silica gel column chromatography with hexane/ethyl acetate as the mobile phase (4:1, v/v) to obtain protected hexanal as a colorless liquid (18.2 g, 90% yield). ^{1}H NMR (400 MHz, $CDCl_3$): δ (ppm) 4.49−4.44 (t, 1H), 3.93−3.89 (dd, 2H), 3.83−3.79 (d, 2H), 3.47−3.42 (dd, 2H), 1.80−1.75 (t, 1H), 1.66−1.59 (m, 2H), 1.45−1.24 (m, 6H), 0.93−0.87 (t, 3H), 0.76−0.72 (s, 3H). ^{13}C NMR (101 MHz, $CDCl_3$): δ (ppm) 102.47, 73.0, 65.88, 34.81, 31.72, 23.59, 22.57, 16.96, 14.0. Electrospray ionization mass spectrometry (ESI-MS): m/z of $[M + Na]^+$ calcd 225.1492; found 225.1459.

Synthesis of Tri(methylene ether)methyl Hexanal Glycidyl Ether (THG) Monomer. In a 250 mL round-bottom flask, 11.3 g (118.6 mmol) of epichlorohydrin and 478 mg (1.48 mmol) of TBAB were mixed and 100 mL of 50% NaOH solution was added in an ice bath at 0 °C. The mixture was then stirred vigorously at 0 °C for 30 min. Subsequently, 6.0 g (29.66 mmol) of protected hexanal was added to the mixture and stirred for 36 h at room temperature. Finally, the reaction mixture was diluted with water and the aqueous phase was extracted using DCM. The organic phase was concentrated under reduced pressure, and the crude product was purified using silica gel column chromatography with hexane/ethyl acetate as the mobile phase (9:1, v/v) to produce THG as a colorless liquid. Finally, THG was subjected to azeotropic distillation to provide the pure product (6.5 g, 85% yield). ^{1}H NMR (400 MHz, $CDCl_3$): δ (ppm) 4.47−4.4 (t, 1H), 3.95−3.84 (ddd, 2H), 3.79−3.72 (dd, 1H), 3.66−3.61 (s, 2H), 3.51−3.43 (dd, 1H), 3.42−3.34 (dd, 2H), 3.19−3.13 (m, 1H), 2.82−2.78 (dd, 1H), 2.64−2.61 (dd, 1H), 1.65−1.56 (dd, 2H), 1.45−1.24 (m, 6H), 0.93−0.85 (t, 3H), 0.75 (s, 3H). ^{13}C NMR (101 MHz, $CDCl_3$): δ (ppm) 102.4, 75.68, 73.60, 72.0, 50.88, 43.90, 34.84, 31.74, 23.69, 22.56, 19.12, 14.03. ESI-MS: m/z of $[M + Na]^+$ calcd 281.1692; found 281.1721.

Copolymerization of THG with PEG_{20k} (P7). The ABA triblock copolymer was synthesized using PEG_{20k} as the macroinitiator. PEG_{20k} (3.0 g, 0.15 mmol) was placed into a Schlenk flask and flame-dried under a high vacuum on a Schlenk line. After charging the flask with nitrogen and adding 6.0 mL of toluene, the resulting solution was stirred for 30 min at 60 °C to dissolve the PEG_{20k}. Next, 375 μL of *t*-BuP_4 (0.80 M, 0.3 mmol) was added to the mixture and stirred for 30 min. The temperature was then decreased to 40 °C, and 348.5 mg (1.35 mmol) of THG was added dropwise to the mixture. After 24 h, 36.6 mg (0.3 mmol) of benzoic acid was added to terminate the polymerization. After diluting the resulting polymer with DCM, the mixture was passed through basic aluminum oxide to remove the residual *t*-BuP_4. The resulting polymer was purified via precipitation in hexane and then filtered and dried under high vacuum to obtain PTHG-*b*-PEG-*b*-PTHG as a white powder (2.9 g, 96% yield). The molecular weight ($M_{n,NMR}$) of the polymer was calculated to be 21,800 g/mol using the NMR spectrum by comparing the peak area of the acetal proton at 4.48 ppm to that of the protons observed in the range of 3.95−3.37 ppm, corresponding to the polyether backbone of PEG and THG blocks (Figure 1). The following equation was used to determine $M_{n,NMR}$: $M_{n,NMR}$ = (molecular weight of the THG monomer) × (number of repeating units) + (molecular weight of PEG_{20k}).

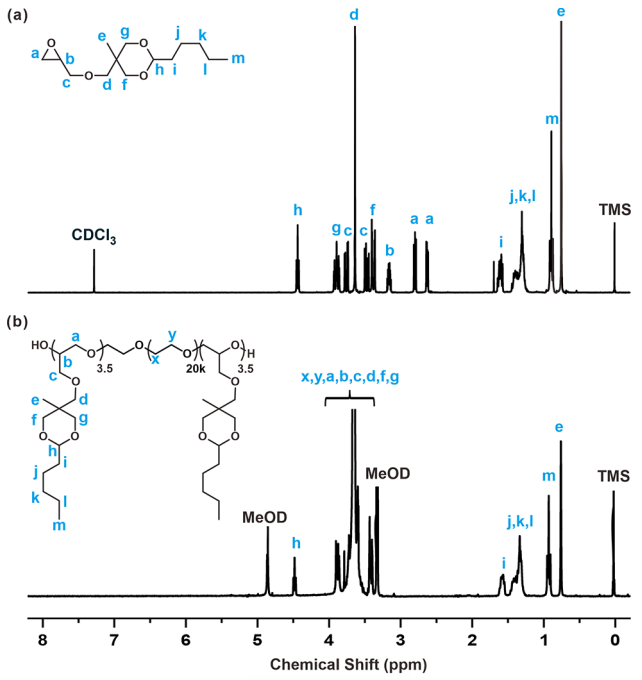

Figure 1. ^{1}H NMR spectra of the (a) THG monomer and (b) $PTHG_{3.5}$-*b*-PEG-*b*-$PTHG_{3.5}$ polymer (P7 in Table 1).

^{1}H NMR (300 MHz, methanol-d_4): δ (ppm) 4.48 (t, 7H), 3.95−3.37 (m, 1898H), 1.64−1.52 (m, 14H), 1.49−1.25 (m, 42H), 0.98−0.88 (t, 21H), 0.76 (s, 21H).

Preparation of the ABA Triblock Copolymer Hydrogels. Different weight percentages of the ABA triblock copolymers were dissolved in 0.10 M phosphate-buffered saline (PBS) at pH 7.4 and allowed to acclimatize for 12 h at 10 °C; for example, 70 mg of P7 was dissolved in 1.0 mL of PBS in a pH 7.4 buffer solution to prepare the 7 wt % P7 hydrogel.

Determination of the Critical Micelle Concentration (CMC) of the Polymers. Various concentrations of the polymer solutions in DMF were prepared, and 10 μL of pyrene solution (5.0 mg/L in DMF) was added to each. The solutions were then vigorously stirred for 30 min at room temperature. Following this, 5.0 mL of deionized water was added to each solution using a syringe pump at a rate of 0.5 mL/min and the solutions were left overnight to equilibrate. The final concentration of pyrene (0.01 mg/L) should be lower than the solubility of pyrene in water at 25 °C (0.135 mg/L). A fluorometer was used to measure the fluorescence of each pyrene-containing polymer micelle solution at an emission wavelength of 372 nm. Plotting the ratio of the fluorescence intensities at 339 and 332 nm against the polymer concentrations was used to determine the critical micelle concentration (CMC) at the inflection point.

Hydrolysis of $PTHG_{3.5}$-*b*-PEG-*b*-$PTHG_{3.5}$ (P7). In the typical process, 100 mg of P7 was taken in a 25 mL round-bottom flask and dissolved in 3 mL of methanol. Following this, 1.5 mL of HCl solution (37%) was added, and the mixture was stirred overnight at room temperature. Finally, the hydrolyzed polymer was purified via precipitation in diethyl ether three times to obtain the hydrolyzed P7 sample as a white powder (80 mg, yield: 80%). ^{1}H NMR (300 MHz, methanol-d_4): δ (ppm) 3.95−3.37 (m, 1898H), 0.90 (d, 21H).

https://doi.org/10.1021/acs.biomac.4c00586
Biomacromolecules XXXX, XXX, XXX−XXX

Scheme 1. Synthesis of the Functional Monomer Tri(methylene ether)methyl Hexanal Glycidyl Ether (THG) and Subsequent Polymerization to Produce the Triblock Copolyether PTHG-*b*-PEG-*b*-PTHG, Followed by Hydrogel Formation and Subsequent Degradation under Acidic Conditions

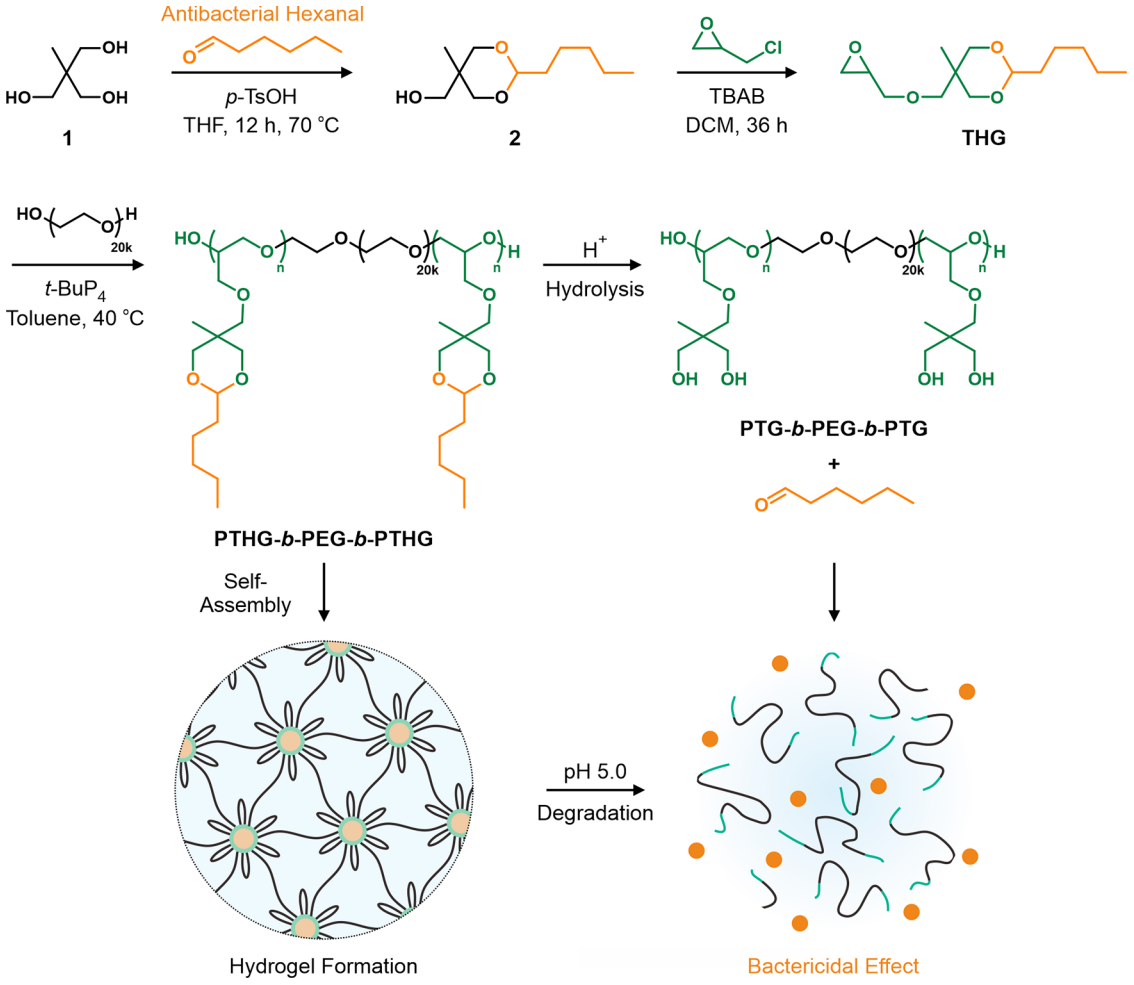

In Vitro Cell Viability Assays. The viability of mouse fibroblast cells (L929 cell line) was measured using 3-(4,5-dimethylthiazol-2-yl)-2,5-diphenyltetrazolium bromide (MTT)-based cytotoxicity assays. L929 cells were grown in Roswell Park Memorial Institute (RPMI)-1640 (with L-glutamine) containing 10% fetal bovine serum (FBS) and 1% antibiotic–antimycotic (penicillin–streptomycin; 10,000 U/mL). The cells were then cultured in a humidified incubator at 37 °C with 5% CO_2 for 48 h and seeded in a 96-well plate at a concentration of 1.5×10^5 cells/mL. After incubation for 24 h, the cells were treated with different concentrations of P7 (0, 25, 50, 100, 250, and 500 μg/mL in a DMSO–water solution; 5:95 v/v) and incubated for 24 h at 37 °C under 5% CO_2. The cells were washed with PBS (pH 7.4) twice and incubated with 100 μL of MTT solution for 4 h at 37 °C. The obtained formazan crystals were then dissolved in DMSO and incubated for 30 min. Finally, the absorbance was measured at 570 nm using a microplate reader (PerkinElmer VICTOR X5), and the results were compared with the control. Similarly, different concentrations of hydrolyzed P7 (0, 25, 50, 100, 250, and 500 μg/mL in deionized water) were used to treat L929 cells to determine the cytotoxicity of hydrolyzed P7 polymer.

Preparation of Hydrogel Extracts for Antibacterial Assays. Initially, 2.0 mL of 7 wt % P7 hydrogel was prepared in deionized water in a 10 mL glass vial and allowed to acclimatize for 12 h at 10 °C. Next, 5 mL of acetate buffer (pH 5.0) solution was added to the hydrogel and incubated at 37 °C. After 4 days, the aqueous solution was extracted, the pH was adjusted to 7.4, and the solution was lyophilized to remove the water. Finally, the lyophilized sample was dissolved in 1.0 mL of pristine tryptic soy broth medium with 10% DMSO to produce the hydrogel extract.

Antibacterial Activity Assays. For the antibacterial activity experiment, both Gram-positive *S. aureus* (25923, ATCC) and Gram-negative *E. coli* (25922, ATCC) were employed as model bacteria. To evaluate the antibacterial effect of the hydrogel sample, we followed a modified version of a previously reported method.[34] Both control and hydrogel extracts were prepared in pristine tryptic soy broth medium with DMSO (5% v/v).

Initially, *S. aureus* and *E. coli* were individually suspended in tryptic soy broth medium (soybean–casein digest medium, Becton Dickinson and Company) and incubated at 37 °C under aerobic conditions. We collected the incubated bacteria by centrifuge and adjusted the concentration of each bacterial suspension to an optical density (OD) of 0.1 by measuring at 600 nm. Then, 1.0 mL of the bacterial suspension was seeded into 24-well plates and incubated at 37 °C under aerobic conditions to create the bacterial exposure conditions. Next, 1.0 mL of the prepared control sample and hydrogel extracts were individually added to each well. Consequently, each well contained a medium with 2.5% v/v DMSO and the concentration of seeded bacteria reached an OD of 0.05. A concentration of 2.5% v/v DMSO was selected for the experiment to ensure that bacterial growth had a minimal influence on the results.[35] Subsequently, the samples were incubated for 6 h at 37 °C. After incubation, the OD value of each well was measured using a microplate reader (λ = 600 nm), and the bacterial concentration was calculated.

Agar Colony Formation Assays. After incubating the hydrogel extract and bacterial mixtures for 6 h, the *E. coli* and *S. aureus*

https://doi.org/10.1021/acs.biomac.4c00586
Biomacromolecules XXXX, XXX, XXX–XXX

Table 1. Characterization Data for All Triblock Copolyethers Synthesized in This Study

code	polymer composition	$M_{n,NMR}$[a] (g/mol)	DP_{NMR}[a]	$M_{n,GPC}$[b] (g/mol)	$Đ$[b]	T_g[c] (°C)	CMC[d] (mg/L)
P7	$PTHG_{3.5}$-*b*-PEG-*b*-$PTHG_{3.5}$	21,800	7	20,200	1.06	−38.9	27.0
P10	$PTHG_5$-*b*-PEG-*b*-$PTHG_5$	22,600	10	20,900	1.05	−43.0	14.0
P14	$PTHG_7$-*b*-PEG-*b*-$PTHG_7$	23,600	14	20,400	1.06	−40.6	9.2

[a]Determined from ^{1}H NMR spectra of the copolyethers. [b]Measured using GPC with THF as the eluent and PEG standards. [c]Measured using DSC at a scan rate of 10 °C/min. [d]Critical micelle concentration, determined using the emission spectra of pyrene with various concentrations of the polymers.

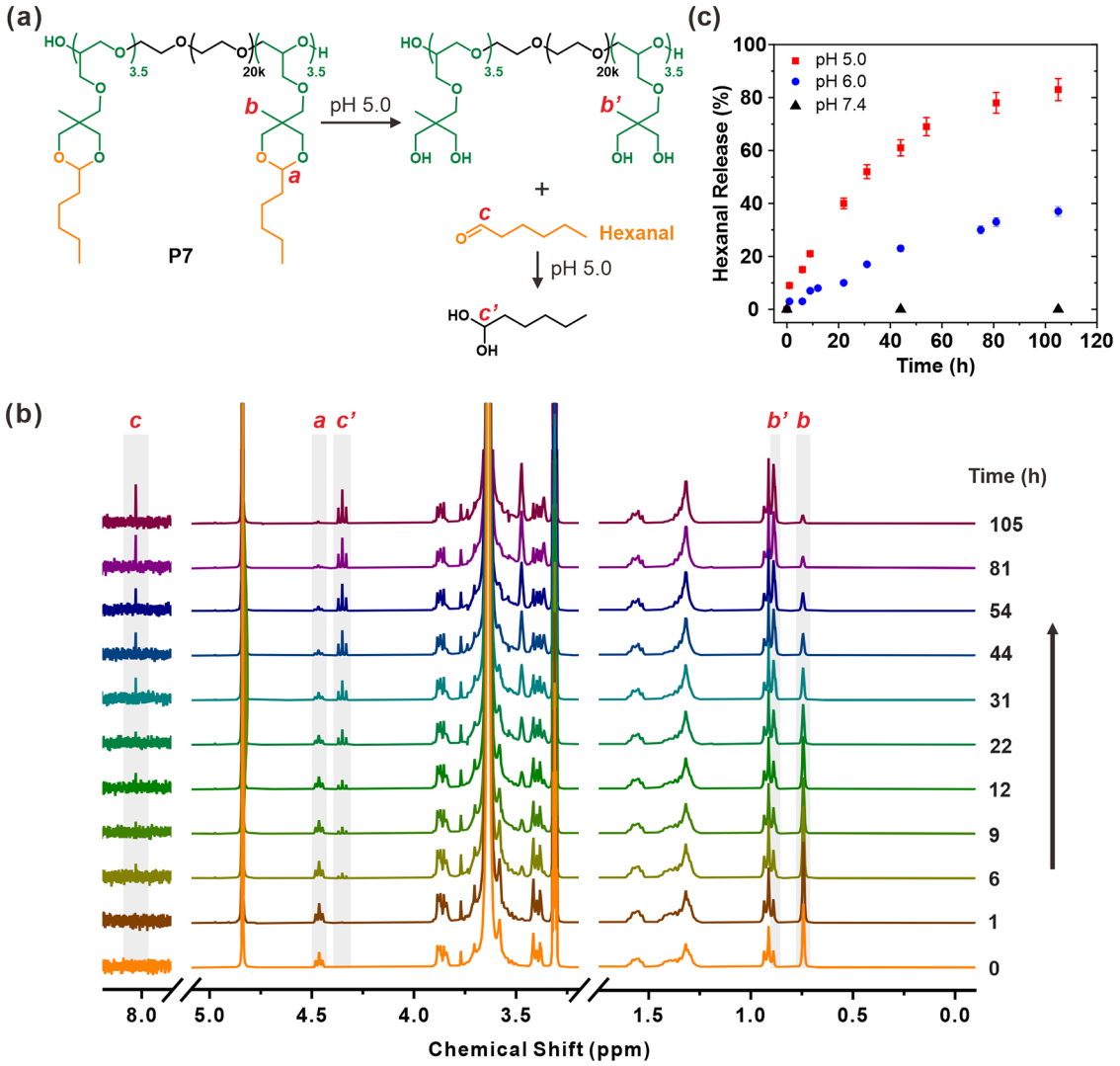

Figure 2. (a) Schematic representation of the degradation of $PTHG_{3.5}$-*b*-PEG-*b*-$PTHG_{3.5}$ (P7 in Table 1) under acidic conditions to yield hydrolyzed P7 with the concomitant release of hexanal, (b) in situ ^{1}H NMR analysis of P7 in CD_3OD (pH 5) over time to monitor the release of hexanal, and (c) percentage of hexanal released from P7 according to the pH and time (n = 3).

solutions were diluted by a factor of 100 and 1000, respectively. Next, 100 μL of the diluted solutions was uniformly spread onto Tryptic Soy agar plates, which were incubated for 16 h for colony formation.[36]

Nile Red Encapsulation and Release Analysis. For Nile Red encapsulation, 1.0 μg of Nile Red and 70 mg of P7 were dissolved in 2 mL of acetonitrile and stirred for 30 min until the acetonitrile evaporated. Next, 1.0 mL of deionized water was added and the mixture was left to stand for 12 h at 10 °C. For the release analysis, 3.0 mL of different pH solutions (pH 5.0, 6.0, and 7.4) were added to as-synthesized hydrogel samples and incubated at 37 °C. Liquid samples were collected at specific times and the absorbance was measured.

RESULTS AND DISCUSSION

The pH-responsive glycidyl ether monomer bearing hexanal moiety through acetal linkage, THG, was synthesized following a two-step reaction pathway. Initially, hexanal was treated with tris(hydroxymethyl)ethane in the presence of *p*-TsOH as a catalyst to afford the protected hexanal (Scheme 1). This conversion was validated by the appearance of a characteristic signal of the acetal moiety at 4.49−4.44 and 102.4 ppm in the ^{1}H and ^{13}C NMR spectra, respectively (Figures S1 and S2). ESI-MS analysis of the protected hexanal revealed a base peak at m/z = 225.14, corresponding to the sodium adduct of the monomer $[M + Na]^+$ (Figure S3). Subsequently, a substitution

https://doi.org/10.1021/acs.biomac.4c00586
Biomacromolecules XXXX, XXX, XXX−XXX

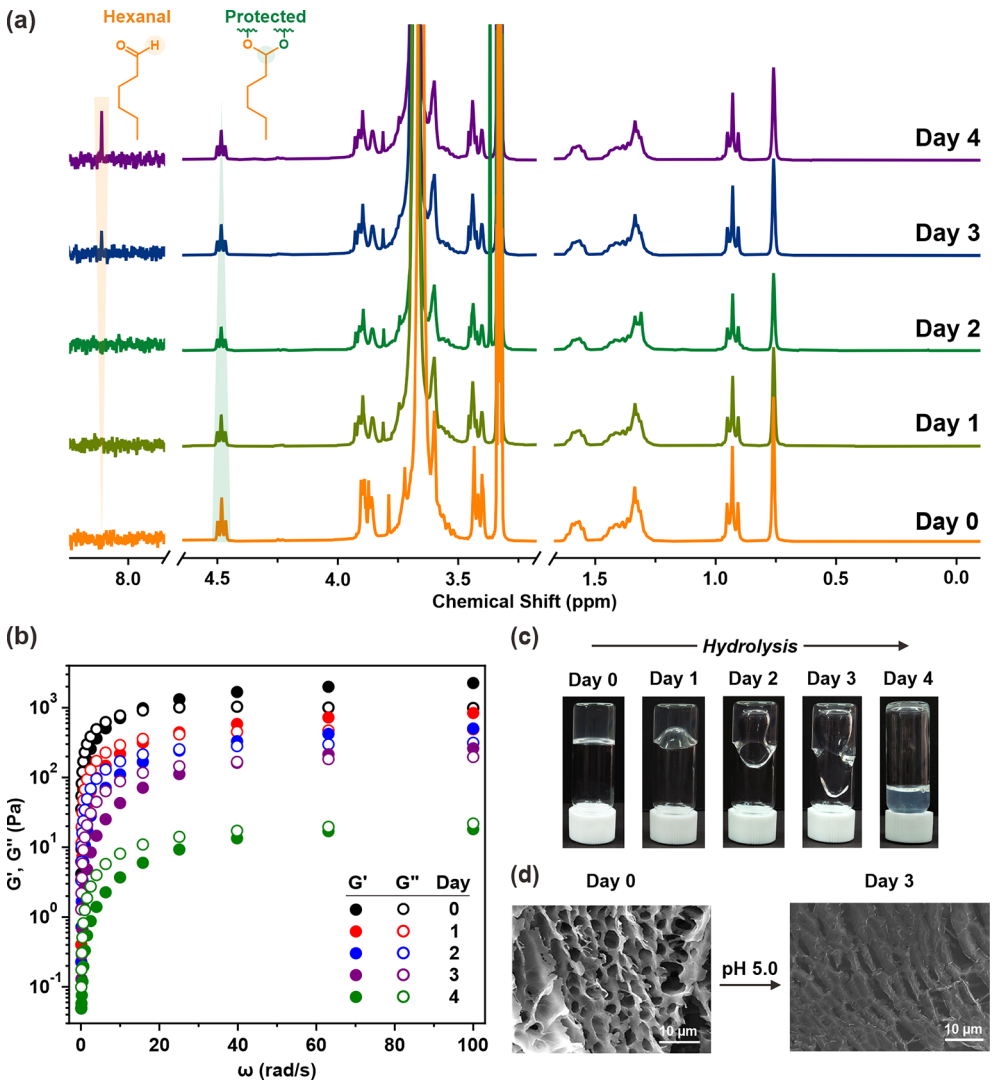

Figure 3. (a) Stacked ^{1}H NMR spectra of 7 wt % P7 in CD_3OD after degradation at pH 5 over time. (b) Storage modulus G' (solid circles) and loss modulus G'' (open circles) of 7 wt % P7 hydrogel after incubation at pH 5 over time and (c) photographs of 7 wt % P7 hydrogel at pH 5 after incubation for different times at 37 °C. Note that prior to taking the photographs, the vials were inverted for 20 s. (d) SEM images of 7 wt % P7 hydrogel before and after incubation at pH 5 for 3 days at 37 °C.

reaction between the protected hexanal and epichlorohydrin yielded the desired monomer THG in an isolated yield of 85% after purification via fractional distillation (Scheme 1). The chemical structure of THG was characterized by different NMR techniques, including ^{1}H and, ^{13}C NMR, heteronuclear single-quantum correlation (HSQC), and ESI-MS (Figures 1a and S4−S6).

In the subsequent step, the ABA triblock copolymers were synthesized via anionic ring-opening polymerization (AROP) at 40 °C for 24 h using PEG_{20k} (M_w = 20 kg/mol) as the macroinitiator and *t*-BuP_4 as the organic superbase. In this study, *t*-BuP_4 was used as the superbase to ensure controlled polymerization under mild reaction conditions. Three different amphiphilic triblock copolymers that differed in the degree of hydrophobicity of the PTHG groups (i.e., $PTHG_n$-*b*-PEG_{20K}-*b*-$PTHG_n$) were synthesized (Table 1). All of the characteristic proton peaks of these triblock copolymers were observed in the corresponding ^{1}H NMR spectra (Figures 1b, S7, and S8). Specifically, the degree of polymerization (DP) and $M_{n,NMR}$ of the triblock copolymers were determined by comparing the peak area of the acetal proton at 4.48 ppm to that of the protons observed in the range of 3.95−3.37 ppm, corresponding to the polyether backbone of the PEG and THG blocks. The ^{13}C NMR spectrum of triblock copolymer (P10) further validated the existence of both THG and PEG blocks (Figure S9). Furthermore, unimodal distributions of the triblock copolymers with a narrow molecular weight dispersity ($Đ$ < 1.06) observed in the gel permeation chromatography (GPC) analysis confirmed the controlled nature of the polymerization (Figure S10 and Table 1). Moreover, differential scanning calorimetry (DSC) analysis revealed a single glass-transition temperature (T_g) for all three triblock copolymers, suggesting a fully miscible nature of the all polyether-based triblock copolymer system (Table 1 and Figure S11). The lack of a significant change in the T_g with an increase in the DP of THG from 7 to 14 was possibly due to the lower fraction of hydrophobic end-blocks compared to the PEG midblock.

To evaluate the self-assembly behavior and micelle stability of the synthesized polymers, the critical micelle concentration (CMC) was determined using pyrene as a fluorescent probe. The CMC was estimated by plotting the ratio of the fluorescence intensity of pyrene incorporated into the

https://doi.org/10.1021/acs.biomac.4c00586
Biomacromolecules XXXX, XXX, XXX−XXX

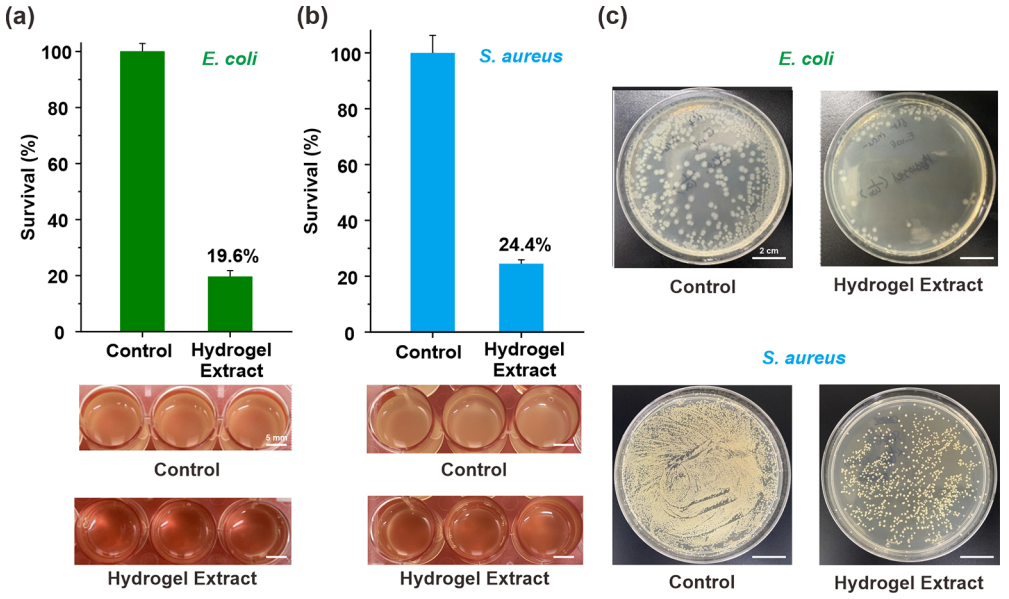

Figure 4. Antibacterial activity evaluation of P7 hydrogel. (a, b) Survival rate for *E. coli* and *S. aureus*, respectively, with hydrogel extract after incubation for 6 h (n = 3). (c) Photographs of *E. coli* and *S. aureus* grown on agar plates in the presence of the P7 extract.

hydrophobic core of micelles at wavelengths 339 and 332 nm against the polymer concentrations. A decrease in the CMC was observed with an increase in the hydrophobicity of the polymers (27.0, 14.0, and 9.2 mg/L for P7, P10, and P14, respectively; Table 1 and Figure S12).

In the next step, the release of hexanal from P7 at various pH levels was monitored using in situ ^{1}H NMR titration experiments (Figure 2). Specifically, P7 was dissolved in CD_3OD in an NMR tube, and the pH of the solution was adjusted to pH 5.0 using HCl solution. The solution was incubated at 37 °C, with the spectrum recorded at different time points. Interestingly, the acetal proton at 4.48 ppm decreased steadily as the incubation time increased, with the generation of two additional peaks at 4.3 and 8.1 ppm (Figure 2b). The peak at 8.1 ppm (peak *c* in Figure 2b) corresponded to the aldehyde peak of the released hexanal in equilibrium with the hydrated form under acidic conditions. In parallel, the control experiment with pristine hexanal in CD_3OD at pH 5.0 clearly revealed that the peak at 4.3 ppm originated from hydrated hexanal forming a diol structure (Figure S13).

In situ ^{1}H NMR experiments were further performed to calculate the percentage of hexanal released over time at different pH levels (Figure 2c). By maintaining the proton peaks for the polyether backbone of P7 at 3.95−3.37 ppm and comparing the integral of the acetal proton at 4.48 ppm with respect to that at 4.30 ppm for the diol structure of hydrated hexanal, the percentage of hexanal released over time was calculated. At pH 5.0, 83% of the hexanal was released after 105 h. In contrast, a release of only 37% was observed at pH 6.0, whereas no noticeable hexanal was detected at pH 7.4 (Figure S14).

In an aqueous medium, the synthesized ABA triblock copolymers self-assembled to generate hydrogels with PTHG cores interconnected by the PEG midblock, as depicted in Scheme 1. Higher polymer concentrations and longer hydrophobic end-blocks are often preferred for the creation of macroscopic 3D hydrogel networks.[37] This demonstrates that the gelation occurs at a specific polymer concentration and DP of hydrophobic end-blocks. To evaluate the concentration threshold for the ABA triblock copolymers in hydrogel formation, several hydrogel samples were prepared by altering the concentrations of P7, P10, and P14 in the range of 3−9 wt % (Figure S15). Based on visual analysis after vial inversion, transparency, and rheological analysis, 7 wt % P7 was found to generate a transparent hydrogel with high mechanical strength (Figure S15). At a temperature of 37 °C, the storage modulus (G') of 7 wt % P7 hydrogel was always higher than the loss modulus (G'') above an angular frequency of 10 rad/s, suggesting the stable gel state of the hydrogels (Figure S15).

In addition, we conducted a dynamic cyclic strain scanning test (γ = 200 and 1%) for periodic cycles of destruction and recovery of the 7 wt % P7 hydrogel to examine the recovery rate for its mechanical strength (Figure S16). When 200% strain was applied to the hydrogel, the G' and G'' values were reversed, indicating a gel-to-sol transition. After repeated trials, G' and G'' exhibited significant reversibility while retaining the necessary stability of the hydrogel.

In line with the hydrogel formation and subsequent degradation, we examined the hydrolysis of the acetal pendants within the hydrogel. Specifically, the ex situ ^{1}H NMR spectra of 7 wt % P7 hydrogel were acquired during incubation for set periods of time at pH 5 and 37 °C (Figure 3a). A decrease in the acetal proton peak at 4.48 ppm and the generation of the aldehyde proton peak for hexanal at 8.2 ppm were observed with an increase in the incubation time. Figure 3b depicts the viscoelastic gel-to-sol transition for 7 wt % P7 hydrogels after incubation in 0.10 M acetate buffer at pH 5 and 37 °C for different periods of time. Initially, the G' value for 7 wt % P7 hydrogel was higher than the G'' value. However, as the incubation time increased, the hydrogel fluidized, as evidenced by the gradual decrease in the G' and G'' values, with an abrupt gel-to-sol transition after 4 days of incubation. To visualize the viscoelastic changes, images of hydrogel samples taken at different incubation times were collected after the inversion of the vials (Figure 3c). In addition, the morphological changes of the hydrogel following incubation at pH 5 were monitored by taking scanning electron microscopy (SEM) images. Figure 3d shows the complete

https://doi.org/10.1021/acs.biomac.4c00586
Biomacromolecules XXXX, XXX, XXX−XXX

disruption of the porous network of P7 hydrogel after incubation for 3 days at pH 5.0, indicating successful hydrogel degradation.

A vital characteristic of biomaterials for potential biomedical applications is biocompatibility. We conducted MTT cytotoxicity assays to evaluate the biocompatibility of P7 with mouse fibroblast cells (L929 cell line) (Figure S17a). Cell viability remained higher than 80% even at P7 concentrations as high as 500 μg/mL, suggesting reasonable biocompatibility. In addition, to test the biocompatibility of the polymer generated after the release of hexanal, we hydrolyzed P7 using HCl solution. The disappearance of the acetal proton peaks at 4.48 ppm from the ^{1}H NMR spectrum indicated successful hydrolysis (Figure S18). The hydrolyzed P7 was found to be completely water-soluble owing to the high fraction of the polyol structures. As expected, hydrolyzed P7 exhibited high biocompatibility and minimal cytotoxicity (Figure S17b).

Furthermore, the antibacterial activity of P7 hydrogel (7 wt %) activated by bacteria-induced microenvironment was assessed. Local environments infected by bacteria undergo acidification due to bacterial growth and colonization. Therefore, to verify the release of hexanal in response to such pH changes, we mimicked an acidic microenvironment and obtained hydrogel extracts under pH 5 conditions. The obtained hydrogel extract was employed instead of the hydrogel itself for three reasons: (1) validation of the antibacterial performance of hydrogel based on a stimuli-triggered antimicrobial release mechanism, (2) evaluation of antibacterial efficacy of solely antimicrobials excluding the influence of pH, utilizing condition of pH 7.3 ± 0.2 optimized for bacterial growth and proliferation, and (3) the volatile nature of released hexanal, posing challenges to precise quantification. The antibacterial analysis included both Gram-positive *S. aureus* and Gram-negative *E. coli* bacteria due to the possibility of differences in sensitivity to antibacterial agents arising from different cell wall structures. After the incubation of bacterial solutions with the hydrogel extract for 6 h, the survival rate was determined by measuring the OD values. *E. coli* and *S. aureus* had low survival percentages of 19.6 and 24.4%, respectively, confirming that the hydrogel had significant antibacterial activity (Figure 4a,b). The inhibitory effect of the hydrogel sample on bacterial growth was supported by the negligible turbidity of the solutions treated with hydrogel extract compared to the control. Subsequent to a 16 h incubation period for colony development, a marked reduction in colony formation was observed in both *E. coli* and *S. aureus* exposed to hydrogel extracts compared to controls (Figure 4c). These results demonstrated that hydrogel can be treated for both bacteria strains by potent antibacterial activity. Our assessment elucidated the release of bacteria-triggered releasing of hexanal and its subsequent antibacterial performance, highlighting the on-demand, self-adaptive antibacterial activity of the hydrogel. This mechanism not only mitigates premature depletion of antimicrobials but also exhibits low cytotoxicity to cells, as antibacterial activation occurs exclusively in the presence of bacterial challenge.

Finally, the degradability of the hydrogel under acidic conditions encourages us to utilize it as a dual-release system in which the pH-triggered release of hexanal promotes gel degradation and simultaneously facilitates the release of an encapsulated model therapeutic agent from the hydrogel matrix. Nile Red was chosen as the model hydrophobic dye that was loaded into 7 wt % P7 hydrogel (Figure 5a). The release of Nile Red was monitored in solutions with a pH of

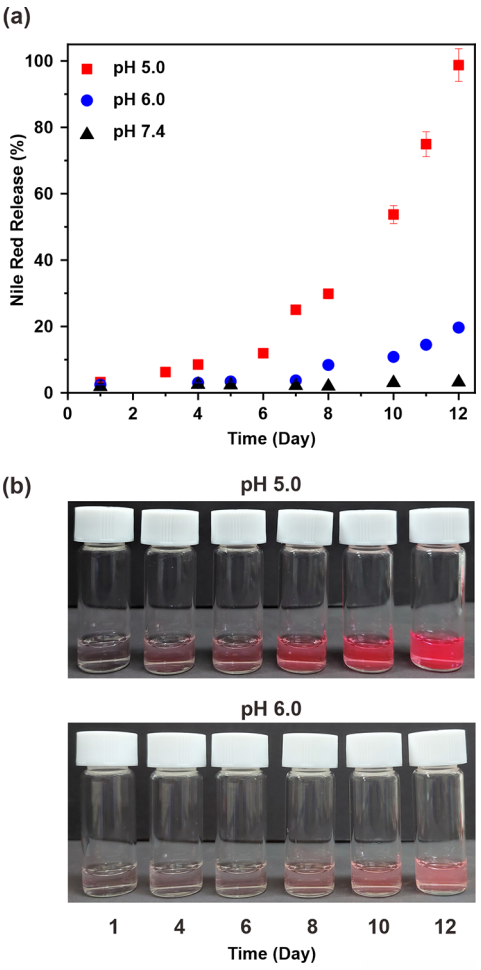

Figure 5. (a) Percentage of Nile Red released from 7 wt % P7 hydrogel at pH 5.0, 6.0, and 7.4 over time and (b) photographic images of the solutions after the release of Nile Red from the hydrogel at pH 5 (top) and pH 6 (bottom) over time.

5.0, 6.0, or 7.4 over time. At pH 5.0, the absorbance of Nile Red at 545 nm gradually increased with the incubation time (Figure S19a,d) with a subsequent change in color from colorless to pink (Figure S19c). However, the release rate was comparatively low at pH 6.0 (Figure S19b,c) and no release was observed at pH 7.4 (Figure S19d). Therefore, the degradation of the hydrogel facilitated the release of the dye under acidic conditions. The amount of Nile Red released was quantified using UV−vis spectroscopy (Figures S20 and S21). A release rate of 99% for Nile Red was observed at pH 5.0 after 12 days of incubation at 37 °C, compared to only 20% at pH 6.0 (Figure 5a,b). Interestingly, no leaching of Nile Red from the hydrogel was observed at pH 7.4. The key feature of this hydrogel is the simultaneous release of both the bioactive aldehyde and dye, triggered by an acidic pH environment. This controlled release can be employed for various applications, particularly in the drug delivery system.

CONCLUSIONS

In brief, we designed and synthesized a polyether-based ABA-type triblock copolymer hydrogel consisting of a hydrophilic

https://doi.org/10.1021/acs.biomac.4c00586
Biomacromolecules XXXX, XXX, XXX−XXX

PEG midblock and hydrophobic end-blocks to which antibacterial hexanal was attached through an acetal linkage. Under acidic conditions, the controlled release of hexanal through the hydrolysis of the acetal pendants triggered hydrogel degradation. Significantly, the released hexanal exhibited remarkable antibacterial efficacy against both *E. coli* and *S. aureus*. The pH-triggered hydrogel degradation was further utilized to release encapsulated Nile Red from the hydrophobic micellar core of the hydrogel in a controlled fashion. By leveraging this dual-release capability of the hydrogel, we anticipate the highly controlled release of multiple therapeutic agents for achieving effective drug delivery hydrogels.

■ ASSOCIATED CONTENT

Supporting Information

The Supporting Information is available free of charge at https://pubs.acs.org/doi/10.1021/acs.biomac.4c00586.

Additional characterization data for monomer and polymers (^{1}H NMR, ^{13}C NMR, ESI-MS, GPC, DSC, CMC determination, MTT assay), additional rheological analyses, and Nile red release assay (PDF)

■ AUTHOR INFORMATION

Corresponding Authors

Jinkee Hong − *Department of Chemical & Biomolecular Engineering, Yonsei University, Seoul 03722, Republic of Korea;* orcid.org/0000-0003-3243-8536; Email: jinkee.hong@yonsei.ac.kr

Byeong-Su Kim − *Department of Chemistry, Yonsei University, Seoul 03722, Republic of Korea;* orcid.org/0000-0002-6419-3054; Email: bskim19@yonsei.ac.kr

Authors

Neha Choudhury − *Department of Chemistry, Yonsei University, Seoul 03722, Republic of Korea*

Seongeun Cho − *Department of Chemical & Biomolecular Engineering, Yonsei University, Seoul 03722, Republic of Korea;* orcid.org/0000-0001-6533-9759

Jinsu Baek − *Department of Chemistry, Yonsei University, Seoul 03722, Republic of Korea;* orcid.org/0000-0002-6393-9176

Complete contact information is available at: https://pubs.acs.org/10.1021/acs.biomac.4c00586

Author Contributions

[§]N.C. and S.C. contributed equally to this work.

Notes

The authors declare no competing financial interest.

■ ACKNOWLEDGMENTS

This work was supported by the National Research Foundation of Korea (NRF-2021R1A2C3004978 and NRF-2021M3H4A1A04092882).

■ REFERENCES

(1) Yang, K.; Han, Q.; Chen, B.; Zheng, Y.; Zhang, K.; Li, Q.; Wang, J. Antimicrobial Hydrogels: Promising Materials for Medical Application. *Int. J. Nanomed.* **2018**, *13*, 2217−2263.

(2) World Health Organization. *Antimicrobial Resistance: Global Report on Surveillance*; World Health Organization, 2014.

(3) Chandel, A. K. S.; Nutan, B.; Raval, I. H.; Jewrajka, S. K. Self-Assembly of Partially Alkylated Dextran-*graft*-poly[(2-dimethylamino)ethyl methacrylate] Copolymer Facilitating Hydrophobic/Hydrophilic Drug Delivery and Improving Conetwork Hydrogel Properties. *Biomacromolecules* **2018**, *19* (4), 1142−1153.

(4) Kumar, A.; Vemula, P. K.; Ajayan, P. M.; John, G. Silver-Nanoparticle-Embedded Antimicrobial Paints Based on Vegetable Oil. *Nat. Mater.* **2008**, *7* (3), 236−241.

(5) Vishwakarma, A.; Dang, F.; Ferrell, A.; Barton, H. A.; Joy, A. Peptidomimetic Polyurethanes Inhibit Bacterial Biofilm Formation and Disrupt Surface Established Biofilms. *J. Am. Chem. Soc.* **2021**, *143* (25), 9440−9449.

(6) Bhattacharjee, B.; Ghosh, S.; Patra, D.; Haldar, J. Advancements in Release-Active Antimicrobial Biomaterials: A Journey from Release to Relief. *Wiley Interdiscip. Rev.: Nanomed. Nanobiotechnol.* **2022**, *14* (1), No. e1745.

(7) Kohanski, M. A.; Dwyer, D. J.; Collins, J. J. How Antibiotics Kill Bacteria: From Targets to Networks. *Nat. Rev. Microbiol.* **2010**, *8* (6), 423−435.

(8) Salomé Veiga, A.; Schneider, J. P. Antimicrobial Hydrogels for the Treatment of Infection. *Pept. Sci.* **2013**, *100* (6), 637−644.

(9) Bai, X.; Lü, S.; Liu, H.; Cao, Z.; Ning, P.; Wang, Z.; Gao, C.; Ni, B.; Ma, D.; Liu, M. Polysaccharides Based Injectable Hydrogel Compositing Bio-Glass for Cranial Bone Repair. *Carbohydr. Polym.* **2017**, *175*, 557−564.

(10) Lee, J. H. Injectable Hydrogels Delivering Therapeutic Agents for Disease Treatment and Tissue Engineering. *Biomater. Res.* **2018**, *22* (1), No. 27, DOI: 10.1186/s40824-018-0138-6.

(11) Vaghani, S. S.; Patel, M. M.; Satish, C. S. Synthesis and Characterization of pH-Sensitive Hydrogel Composed of Carboxymethyl Chitosan for Colon Targeted Delivery of Ornidazole. *Carbohydr. Res.* **2012**, *347* (1), 76−82.

(12) Wang, X.; Shan, M.; Zhang, S.; Chen, X.; Liu, W.; Chen, J.; Liu, X. Stimuli-Responsive Antibacterial Materials: Molecular Structures, Design Principles, and Biomedical Applications. *Adv. Sci.* **2022**, *9* (13), No. e2104843.

(13) Li, Y.; Han, Y.; Li, H.; Niu, X.; Zhang, D.; Wang, K. Antimicrobial Hydrogels: Potential Materials for Medical Application. *Small* **2024**, *20* (5), No. e2304047.

(14) Wei, T.; Yu, Q.; Chen, H. Responsive and Synergistic Antibacterial Coatings: Fighting against Bacteria in a Smart and Effective Way. *Adv. Healthcare Mater.* **2019**, *8* (3), No. e1801381.

(15) Wang, Z.; Liu, X.; Duan, Y.; Huang, Y. Infection Microenvironment-Related Antibacterial Nanotherapeutic Strategies. *Biomaterials* **2022**, *280*, No. 121249.

(16) Tang, Y.; Xu, H.; Wang, X.; Dong, S.; Guo, L.; Zhang, S.; Yang, X.; Liu, C.; Jiang, X.; Kan, M.; et al. Advances in Preparation and Application of Antibacterial Hydrogels. *J. Nanobiotechnol.* **2023**, *21* (1), No. 300, DOI: 10.1186/s12951-023-02025-8.

(17) Ahmed, W.; Zhai, Z.; Gao, C. Adaptive Antibacterial Biomaterial Surfaces and Their Applications. *Mater. Today Bio* **2019**, *2*, No. 100017.

(18) Wang, J.; Chen, X.-Y.; Zhao, Y.; Yang, Y.; Wang, W.; Wu, C.; Yang, B.; Zhang, Z.; Zhang, L.; Liu, Y.; et al. pH-Switchable Antimicrobial Nanofiber Networks of Hydrogel Eradicate Biofilm and Rescue Stalled Healing in Chronic Wounds. *ACS Nano* **2019**, *13* (10), 11686−11697.

(19) Xu, X.; Huang, Z.; Huang, Z.; Zhang, X.; He, S.; Sun, X.; Shen, Y.; Yan, M.; Zhao, C. Injectable, NIR/pH-Responsive Nanocomposite Hydrogel as Long-Acting Implant for Chemophotothermal Synergistic Cancer Therapy. *ACS Appl. Mater. Interfaces* **2017**, *9* (24), 20361−20375.

(20) Liu, B.; Thayumanavan, S. Substituent Effects on the pH Sensitivity of Acetals and Ketals and Their Correlation with Encapsulation Stability in Polymeric Nanogels. *J. Am. Chem. Soc.* **2017**, *139* (6), 2306−2317.

(21) Hwang, E.; Kim, K.; Lee, C. G.; Kwon, T.-H.; Lee, S.-H.; Min, S. K.; Kim, B.-S. Tailorable Degradation of pH-Responsive All-Polyether Micelles: Unveiling the Role of Monomer Structure and

Hydrophilic−Hydrophobic Balance. *Macromolecules* **2019**, *52* (15), 5884−5893.
(22) Song, J.; Palanikumar, L.; Choi, Y.; Kim, I.; Heo, T.-y.; Ahn, E.; Choi, S.-H.; Lee, E.; Shibasaki, Y.; Ryu, J.-H.; Kim, B. S. The Power of the Ring: A pH-Responsive Hydrophobic Epoxide Monomer for Superior Micelle Stability. *Polym. Chem.* **2017**, *8* (46), 7119−7132.
(23) Son, I.; Lee, Y.; Baek, J.; Park, M.; Han, D.; Min, S. K.; Lee, D.; Kim, B.-S. Ph-Responsive Amphiphilic Polyether Micelles with Superior Stability for Smart Drug Delivery. *Biomacromolecules* **2021**, *22* (5), 2043−2056.
(24) Kissel, T.; Li, Y.; Unger, F. ABA-Triblock Copolymers from Biodegradable Polyester A-blocks and Hydrophilic Poly(ethylene oxide) B-blocks as a Candidate for *in situ* Forming Hydrogel Delivery Systems for Proteins. *Adv. Drug Delivery Rev.* **2002**, *54* (1), 99−134.
(25) Hong, Y.; Kim, J.-M.; Jung, H.; Park, K.; Hong, J.; Choi, S.-H.; Kim, B.-S. Facile Synthesis of Poly(ethylene oxide)-Based Self-Healable Dynamic Triblock Copolymer Hydrogels. *Biomacromolecules* **2020**, *21* (12), 4913−4922.
(26) Baek, J.; Kim, S.; Son, I.; Choi, S.-H.; Kim, B.-S. Hydrolysis-Driven Viscoelastic Transition in Triblock Copolyether Hydrogels with Acetal Pendants. *ACS Macro Lett.* **2021**, *10* (8), 1080−1087.
(27) Baek, J.; Song, N.; Yoo, B.; Lee, W.; Kim, B.-S. Precisely Programmable Degradation and Drug Release Profiles in Triblock Copolyether Hydrogels with Cleavable Acetal Pendants. *J. Am. Chem. Soc.* **2024**, *146* (20), 13836−13845.
(28) Chen, B.-M.; Cheng, T.-L.; Roffler, S. R. Polyethylene Glycol Immunogenicity: Theoretical, Clinical, and Practical Aspects of Anti-Polyethylene Glycol Antibodies. *ACS Nano* **2021**, *15* (9), 14022−14048.
(29) Patel, M.; Park, J. K.; Jeong, B. Rediscovery of Poly(ethylene glycol)s as a Cryoprotectant for Mesenchymal Stem Cells. *Biomater. Res.* **2023**, *27*, No. 17, DOI: 10.1186/s40824-023-00356-z.
(30) Fadida, T.; Selilat-Weiss, A.; Poverenov, E. N-hexylimine-chitosan, a Biodegradable and Covalently Stabilized Source of Volatile, Antimicrobial Hexanal. Next Generation Controlled-Release System. *Food Hydrocolloids* **2015**, *48*, 213−219.
(31) Nakamura, S.; Hatanaka, A. Green-Leaf-Derived C6-Aroma Compounds with Potent Antibacterial Action That Act on Both Gram-Negative and Gram-Positive Bacteria. *J. Agric. Food Chem.* **2002**, *50* (26), 7639−7644.
(32) Song, J.; Hildebrand, P. D.; Fan, L.; Forney, C. F.; Renderos, W. E.; Campbell-Palmer, L.; Doucette, C. Effect of Hexanal Vapor on the Growth of Postharvest Pathogens and Fruit Decay. *J. Food Sci.* **2007**, *72* (4), M108−M112.
(33) U. S. Food and Drug Administration. Hexanal, CAS Reg. No.: 66-25-1, 2024. https://www.cfsanappsexternal.fda.gov/scripts/fdcc/index.cfm?set=FoodSubstances&sort=Sortterm_ID&order=ASC&startrow=1&type=basic&search=hexanal (accessed March 25, 2024).
(34) Choi, M.; Park, S.; Park, K.; Jeong, H.; Hong, J. Nitric Oxide Delivery Using Biocompatible Perfluorocarbon Microemulsion for Antibacterial Effect. *ACS Biomater. Sci. Eng.* **2019**, *5* (3), 1378−1383.
(35) Álvarez-Paino, M.; Muñoz-Bonilla, A.; López-Fabal, F.; Gómez-Garcés, J. L.; Heuts, J. P.; Fernández-García, M. Effect of Glycounits on the Antimicrobial Properties and Toxicity Behavior of Polymers Based on Quaternized DMAEMA. *Biomacromolecules* **2015**, *16* (1), 295−303.
(36) Jeong, H.; Park, J.-H.; Shin, J. H.; Yoo, J.-C.; Park, C. Y.; Hong, J. Prolonged Release Period of Nitric Oxide Gas for Treatment of Bacterial Keratitis by Amine-Rich Polymer Decoration of Nanoparticles. *Chem. Mater.* **2018**, *30* (23), 8528−8537.
(37) Li, J.; Mooney, D. J. Designing Hydrogels for Controlled Drug Delivery. *Nat. Rev. Mater.* **2016**, *1* (12), No. 16071, DOI: 10.1038/natrevmats.2016.71.

https://doi.org/10.1021/acs.biomac.4c00586
Biomacromolecules XXXX, XXX, XXX−XXX